Nucleon resonances with double polarization observables of pion photoproduction

D. Dutta,[1] H. Gao,[1] and T.-S. H. Lee[2]

[1]*Laboratory for Nuclear Science and Department of Physics, Massachusetts Institute of Technology, Cambridge, Massachusetts 02139*
[2]*Physics Division, Argonne National Laboratory, Argonne, Illinois 60439*

The role of the nucleon resonances in the double polarization observables of pion photoproduction is investigated by using the resonance parameters predicted by Capstick and Roberts. As an example, we show that the not-well-determined two-star resonance $N_{3/2}^{-}(1960)$ can be examined by performing experiments on beam-recoil polarization at large angles.

I. INTRODUCTION

Constituent quark models have been widely used to predict the properties of baryon resonances. However, a large number of resonance states which appear in the constituent quark models have not been observed in pion-nucleon scattering. It has been argued [1] that such "missing resonances" either decouple from the pion-nucleon channel or are masked by the neighboring resonances which have large πN decay widths. This has led to suggestions that other reaction channels such as vector meson production [2–4] might be more sensitive to these missing states. However, all possibilities have not been exhausted in the πN channel. One such possibility is to consider the polarization observables. While efforts [5] are being made to measure the single polarizations, it will be interesting to explore double polarizations which could be more effective in revealing some of the missing resonances through interference between the resonant and background (nonresonant) amplitudes. Investigation of these double polarization observables is timely and topical as they coincide with the availability of new opportunities to measure them at Jefferson Lab and other laboratories.

As a step in this direction, we will explore in this paper how the double polarization observables of pion photoproduction can be used to investigate nucleon resonances in the higher-energy region ($1.6 < E < 2.1$ GeV) in which a lot of missing resonances have been suggested. In this energy region, a complete dynamical approach to pion photoproduction, such as that developed [6] in the investigation of the Δ resonance, is still being developed. The main difficulty is due to the large number of resonance states and the complexities of the couplings between several meson-baryon channels. For our present, very limited purpose, we will introduce some rather drastic simplifications in using a formulation which is a direct extension of the dynamical formulation of Ref. [6]. This will then allow us to address the question concerning the missing resonances by relating the resonant amplitude directly to the predictions from a constituent quark model. As an example, we will consider the predictions by Capstick and Roberts [7,8].

In Sec. II, we will give explicitly the formulation used in our calculations. Our findings will be discussed in Sec. III.

II. FORMULATION

The differential cross section of $\gamma N \rightarrow \pi N$ in the center-of-mass (c.m.) frame can be written as

$$\frac{d\sigma}{d\Omega} = \frac{1}{4} \sum_{\lambda_\gamma} \sum_{m_f m_i} |A_{m_f,m_i,\lambda_\gamma}(\mathbf{q},\mathbf{k})|^2, \tag{1}$$

where $\mathbf{k}$ and $\mathbf{q}$ are, respectively, the momenta of the incident photon and outgoing pion, and m_i, m_f, and λ_γ are the spin projections of the initial nucleon, final nucleon, and incoming photon, respectively. For a total invariant mass $W = \sqrt{s}$, the momenta $k = |\mathbf{k}|$ and $q = |\mathbf{q}|$ are

$$k = \frac{1}{2\sqrt{s}}[s - M_N^2],$$

$$q = \frac{1}{2\sqrt{s}}[(s - M_N^2 - M_\pi^2)^2 - 4M_N^2 M_\pi^2]^{1/2},$$

where M_N and M_π are the masses for the nucleon and pion, respectively. The photon laboratory energy E_γ is

$$E_\gamma = \frac{1}{2M_N}[s - M_N^2]. \tag{2}$$

Following the formulation of Ref. [4], we write the pion photoproduction amplitude as

$$A_{m_f,m_i,\lambda_\gamma}(\mathbf{q},\mathbf{k}) = A_{m_f,m_i,\lambda_\gamma}^{(b.g.)}(\mathbf{q},\mathbf{k}) + \sum_{N^*} [A_{m_f,m_i,\lambda_\gamma}^{N^*}(\mathbf{q},\mathbf{k})]. \tag{3}$$

In this work, we assume that the total amplitude $A(\mathbf{q},\mathbf{k})$ of Eq. (3) can be calculated from the multipole amplitude generated by the SAID program [9]. These empirical amplitudes are obtained by the following procedure. For each partial wave, the multipole amplitude is written as a sum of the conventional Born term, vector-meson exchange, and a many-parameter phenomenological term. The amplitudes are unitarized by using the empirical πN phase shifts which are also available in the SAID program. The empirical pion photoproduction multipole amplitude is then obtained by adjusting the parameters of the phenomenological term to perform χ^2 fits to all of the existing data of $\gamma p \rightarrow \pi^+ n$, $\gamma n \rightarrow \pi^- p$ and $\gamma p \rightarrow \pi^0 p$ reactions from threshold up to invariant mass $W = 2.1$ GeV. In this work we use the SM01 solutions [9] from their energy-dependent fits. More details about the SAID program can be found in Refs. [9,10].

TABLE I. Parameters for positive parity nucleon resonances from Refs. [7,8]. The helicity amplitude A_λ is given in units of 10^{-3} GeV$^{-1/2}$. $G(L)$ is in units of MeV$^{1/2}$. The resonance mass M_R^J is in units of MeV.

N^*	M_R^J	$A_{1/2}$	$A_{3/2}$	$G(1)$	PDG [12]
$N\frac{1}{2}^+$	1540	4	—	20.3	$P_{11}(1440)$****
$N\frac{1}{2}^+$	1770	13	—	4.2	$P_{11}(1770)$***
$N\frac{1}{2}^+$	1880	0	—	2.7	
$N\frac{1}{2}^+$	1975	−12	—	2.0	
				$G(1)$	
$N\frac{3}{2}^+$	1795	−11	−31	14.1	$P_{13}(1720)$****
$N\frac{3}{2}^+$	1870	−2	−15	6.1	$P_{13}(1900)$**
$N\frac{3}{2}^+$	1910	−21	−27	1.0	
$N\frac{3}{2}^+$	1950	−5	2	4.1	
$N\frac{3}{2}^+$	2030	−9	15	1.8	
				$G(3)$	
$N\frac{5}{2}^+$	1770	−38	56	6.6	$F15(1680)$****
$N\frac{5}{2}^+$	1980	−11	−6	1.3	
$N\frac{5}{2}^+$	1995	−18	1	0.9	$F_{15}(2000)$**
				$G(3)$	
$N\frac{7}{2}^+$	1980	−1	−2	2.4	$F_{17}(1990)$**
$N\frac{7}{2}^+$	2390	−14	−11	4.9	
$N\frac{7}{2}^+$	2410	+1	−1	0.4	
				$G(5)$	
$N\frac{9}{2}^+$	2345	−29	+13	3.6	$H_{19}(2220)$****

TABLE II. Parameters for negative parity nucleon resonances from Refs. [7,8]. The units are the same as in Table I.

N^*	M_R^J	$A_{1/2}$	$A_{3/2}$	$G(0)$	PDG [12]
$N\frac{1}{2}^-$	1460	+76	—	14.7	$S_{11}(1535)$****
$N\frac{1}{2}^-$	1535	+54	—	12.2	$S_{11}(1650)$****
$N\frac{1}{2}^-$	1945	+12	—	5.7	
$N\frac{1}{2}^-$	2030	+20	—	3.7	
				$G(2)$	
$N\frac{3}{2}^-$	1495	−15	134	8.6	$D_{13}(1520)$****
$N\frac{3}{2}^-$	1625	−33	−3	5.8	$D_{13}(1700)$***
$N\frac{3}{2}^-$	1960	+36	−43	8.2	$D_{13}(2080)$**
$N\frac{3}{2}^-$	2055	+16	0	6.2	
$N\frac{3}{2}^-$	2095	−9	−14	0.2	
				$G(2)$	
$N\frac{5}{2}^-$	1630	2	3	5.3	$D_{15}(1675)$***
$N\frac{5}{2}^-$	2080	−3	−14	5.1	
$N\frac{5}{2}^-$	2095	−2	−6	5.2	$D_{15}(2200)$**
				$G(4)$	
$N\frac{7}{2}^-$	2090	−34	+28	6.9	$G_{17}(2190)$****
$N\frac{7}{2}^-$	2205	−16	+4	4.0	
				$G(4)$	
$N\frac{9}{2}^-$	2215	0	+1	2.5	$G_{19}(2250)$****

Following the formulation of Ref. [6], we write the resonant amplitude as

$$A^{N^*}_{m_f,m_i,\lambda_\gamma}(\mathbf{q},\mathbf{k}) = \frac{1}{2\pi}\frac{M_N}{\sqrt{s}}\sqrt{\frac{q}{k}}I^{N^*}_{m_f,m_\pi,\lambda_\gamma}(\mathbf{q},\mathbf{k}),$$

$$I^{N^*}_{m_f,m_i,\lambda_\gamma}(\mathbf{q},\mathbf{k})$$

$$= \sum_{J,M_J}\frac{\mathcal{M}_{N^*\to N'\pi}(\mathbf{q};m_f;J,M_J)\mathcal{M}_{\gamma N\to N^*}(\mathbf{k};m_i,\lambda_\gamma;J,M_J)}{\sqrt{s}-M_R^J+\frac{i}{2}\Gamma^J(s)},$$
(4)

where M_R^J is the mass of a N^* with spin quantum numbers (J,M_J). Here we neglect the effect due to the nonresonant mechanisms on the N^* decay amplitude and the shift of the resonance position. Then the resonance mass M_R^J and the N^* decay amplitude $\mathcal{M}_{N^*\to\gamma N,\pi N}$ can be identified with the predictions from a quark model, as discussed in Refs. [6,11].

We however do not have information about the total decay width $\Gamma^J(s)$ for most of the N^*'s considered here. For simplicity, we assume that its energy dependence is similar to the width of the $N^*\to\pi N$ decay within the oscillator con-

stituent quark model. Following Ref. [11] and neglecting the real part of the mass shift, we then have

$$\Gamma^J(s) = \Gamma_0^J\frac{\rho(q)}{\rho(q_0)}\left(\frac{q}{q_0}\right)^{2L}\exp[2(\mathbf{q}_0^2-\mathbf{q}^2)/\Lambda^2],$$
(5)

where L is the orbital angular momentum of the considered πN state and

$$\rho(q) = \frac{qE_N(q)E_\pi(q)}{E_N(q)+E_\pi(q)}.$$
(6)

In the above equations, $q(\equiv|\mathbf{q}|)$ is the pion momentum at energy $\sqrt{s}$ while the on-shell momentum q_0 is evaluated at $\sqrt{s}=M_R^J$. The energies are defined by $E_N(q)=\sqrt{M_N^2+\mathbf{q}^2}$ and $E_\pi(q)=\sqrt{M_\pi^2+\mathbf{q}^2}$. Our choice of the total average width Γ_0^J and cutoff parameter Λ for Eq. (5) will be specified in Sec. III.

By setting the photon momentum in the z direction, the $\gamma N\to N^*$ amplitude ($\mathcal{M}_{\gamma N\to N^*}$) in Eq. (4) can be calculated from the helicity amplitude A_λ listed in Ref. [7]:

$$\mathcal{M}_{\gamma N\to N^*}(\mathbf{k};m_i,\lambda_\gamma;J,M_J) = \sqrt{2k}A_{M_J}\delta_{M_J,\lambda_\gamma+m_i}.$$
(7)

The $N^*\to\pi N$ amplitude ($\mathcal{M}_{N^*\to N'\pi}$) takes the following form [13]:

TABLE III. Parameters for positive parity delta resonances from Refs. [7,8]. The helicity amplitude A_λ is given in units of 10^{-3} GeV$^{-1/2}$. $G(L)$ is in units of MeV$^{1/2}$. The resonance mass M_R^J is in units of MeV.

Δ^*	M_R^J	$A_{1/2}$	$A_{3/2}$	$G(1)$	PDG [12]
$\Delta\frac{1}{2}^+$	1835	-31	—	3.9	
$\Delta\frac{1}{2}^+$	1875	-8	—	9.4	$P_{31}(1910)$****
				$G(1)$	
$\Delta\frac{3}{2}^+$	1232	108	186	10.4	$P_{33}(1232)$****
$\Delta\frac{3}{2}^+$	1795	30	51	8.7	$P_{33}(1920)$**
$\Delta\frac{3}{2}^+$	1915	13	14	4.2	
$\Delta\frac{3}{2}^+$	1985	6	3	3.3	
				$G(3)$	
$\Delta\frac{5}{2}^+$	1910	26	-1	3.4	$F_{15}(1905)$****
$\Delta\frac{5}{2}^+$	1990	-10	-28	1.2	$F_{35}(2000)$**
				$G(3)$	
$\Delta\frac{7}{2}^+$	1940	-33	-42	7.1	$F_{37}(1950)$****
$\Delta\frac{7}{2}^+$	2370	-33	-42	1.5	$F_{37}(1950)$****
$\Delta\frac{7}{2}^+$	2460	24	30	1.1	
				$G(5)$	
$\Delta\frac{9}{2}^+$	2420	0	0	1.2	H_{39}
$\Delta\frac{9}{2}^+$	2505	0	0	0.4	

TABLE IV. Parameters for negative parity delta resonances from Refs. [7,8]. The units are the same as in Table III.

Δ^*	M_R^J	$A_{1/2}$	$A_{3/2}$	$G(0)$	PDG [12]
$\Delta\frac{1}{2}^-$	1555	81	—	5.1	$S_{31}(1620)$****
$\Delta\frac{1}{2}^-$	2035	20	—	1.2	$S_{31}(1900)$**
$\Delta\frac{1}{2}^-$	2140	4	—	3.1	
				$G(2)$	
$\Delta\frac{3}{2}^-$	1620	82	68	4.9	$D_{33}(1700)$****
$\Delta\frac{3}{2}^-$	2080	-20	-6	2.2	
$\Delta\frac{3}{2}^-$	2145	0	10	2.2	
				$G(2)$	
$\Delta\frac{5}{2}^-$	2155	11	19	5.2	$D_{35}(1930)$***
$\Delta\frac{5}{2}^-$	2165	0	0	0.6	
$\Delta\frac{5}{2}^-$	2265	0	0	2.4	
$\Delta\frac{5}{2}^-$	2325	0	0	0.1	
				$G(4)$	
$\Delta\frac{7}{2}^-$	2230	14	-4	2.1	G_{37}
$\Delta\frac{7}{2}^-$	2295	0	0	1.8	
				$G(4)$	
$\Delta\frac{9}{2}^-$	2295	-14	-17	4.8	G_{39}

$$\mathcal{M}_{N^* \to N'\pi}(\mathbf{q}; m_f; J, M_J)$$

$$= 2\pi \sqrt{\frac{2M_R^J}{M_N|\mathbf{q}_0|}} \sum_{m_L} \left\langle Lm_L \frac{1}{2}, m_f \middle| J m_J \right\rangle$$

$$\times Y_{Lm_L}(\hat{q}) G(L)(|\mathbf{q}|/|\mathbf{q}_0|)^L f(\mathbf{q}, \mathbf{q}_0), \qquad (8)$$

where $\mathbf{q}_0$ is the π meson momentum at $\sqrt{s} = M_R^J$. Here we also include an extrapolation factor $f(\mathbf{q}, \mathbf{q}_0) = \exp[(\mathbf{q}_0^2 - \mathbf{q}^2)/\Lambda^2]$ similar to that for defining the width, Eq. (5).

By using the information in Refs. [7,8,13], we can get the helicity amplitude A_λ of Eq. (7) and partial-wave transition strength $G(L)$ of Eq.(8) predicted by Capstick and Roberts. The resulting values for the considered 30 N^* and 26 Δ^* are listed in Tables I–IV.

III. RESULTS AND DISCUSSIONS

Our first task is to calculate the resonant amplitude defined by Eqs. (4)–(8). With the helicity amplitude A_λ and partial-wave transition strength $G(L)$ given in Tables I–IV, this amplitude depends only on the choice of the total width Γ_0^J and the cutoff Λ in Eqs. (5) and (8). For simplicity, we set $\Lambda = 650$ MeV for all resonances considered. This value is close to what was determined in the investigation of $\Delta \to \pi N$ [6]. The widths of the known N^* resonances listed in [12] range from 200 to 400 MeV. We therefore take their average value and set $\Gamma_0^J = 300$ MeV for all N^* resonances listed in Tables I and II. For a similar reason, we set $\Gamma_0^J = 120$ MeV for the considered Δ^* resonances listed in
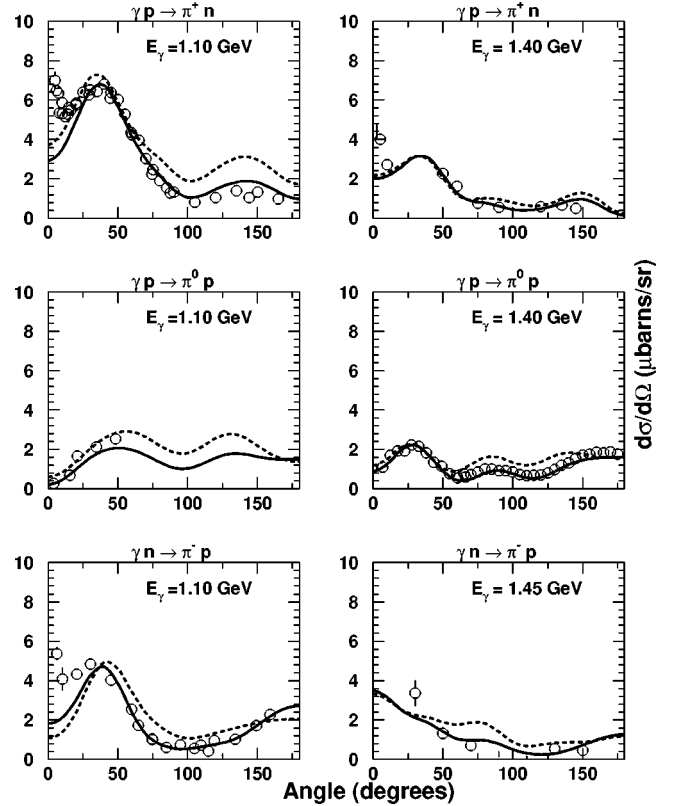

FIG. 1. The differential cross sections of $\gamma N \to \pi N$ reactions calculated from the background amplitude defined by Eq. (9) (dashed curves) and from the SAID amplitude (solid curves) are compared. The data were obtained from Ref. [15].
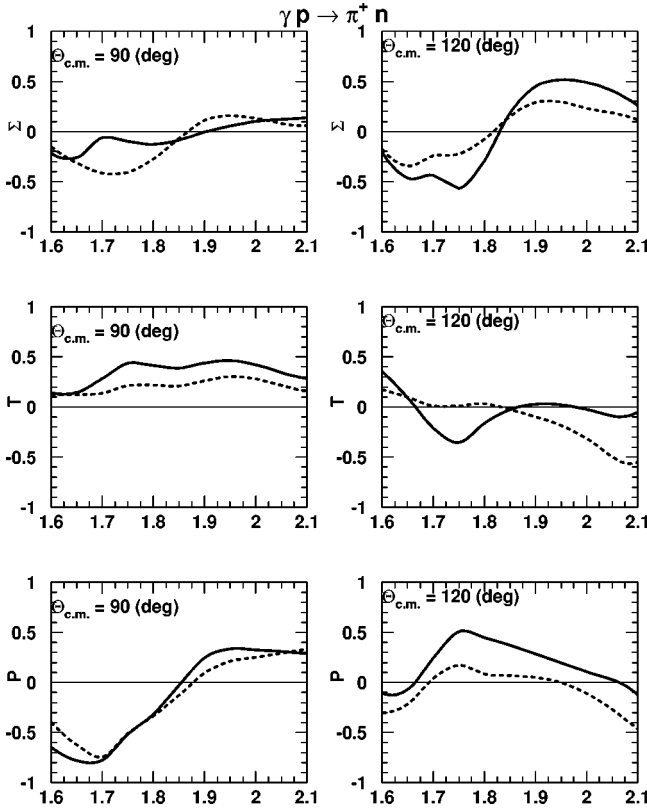
FIG. 2. The single polarization observables: γ asymmetry (Σ), the target asymmetry (T), and the recoil asymmetry (P) at c.m. angles 90° and 120°. The solid (dashed) curves are obtained from using the SAID amplitude [the background amplitude defined by Eq. (9)].

FIG. 3. The beam-target polarization C_{zy}^{BT} with photon helicity = +1 at c.m. angles 90° and 120°. The solid (dashed) curves are obtained from using the SAID amplitude [the background amplitude defined by Eq. (9)].

Tables III and IV. With these specifications, the resonant amplitude, Eq. (4), can be computed with no adjustable parameters. Since the full amplitude $A(\mathbf{q},\mathbf{k})$ is taken from the SAID program, the nonresonant (background) amplitude $A^{(bg)}$ for our investigation can then be fixed by

$$A^{(bg)}_{mf,mi,\lambda_\gamma}(\mathbf{q},\mathbf{k}) = A_{mf,mi,\lambda_\gamma}(\mathbf{q},\mathbf{k}) - \sum_{N^*,\Delta^*} [A^{N^*}_{m_f,m_i,\lambda_\gamma}(\mathbf{q},\mathbf{k})]. \quad (9)$$

With the background amplitude defined above, we then use Eq. (2) to investigate the role of each resonance in determining the resonance amplitude. In Fig. 1, we first observe that the differential cross sections (solid curves) calculated from the employed SAID amplitude agree well with the available data. The dashed curves are obtained when the effects due to all of the considered 56 resonance states are removed. We see that the nucleon resonance effects on the unpolarized differential cross sections are not very pronounced. Furthermore, none of the considered resonances listed in Tables I–IV dominate the difference between the full calculation (solid curves) and the background-only calculation (dashed curves). Obviously, it is not easy to investigate the nucleon resonances by only considering the unpolarized differential cross sections. This is similar to the finding of Ref. [4] in an investigation of ω photoproduction.
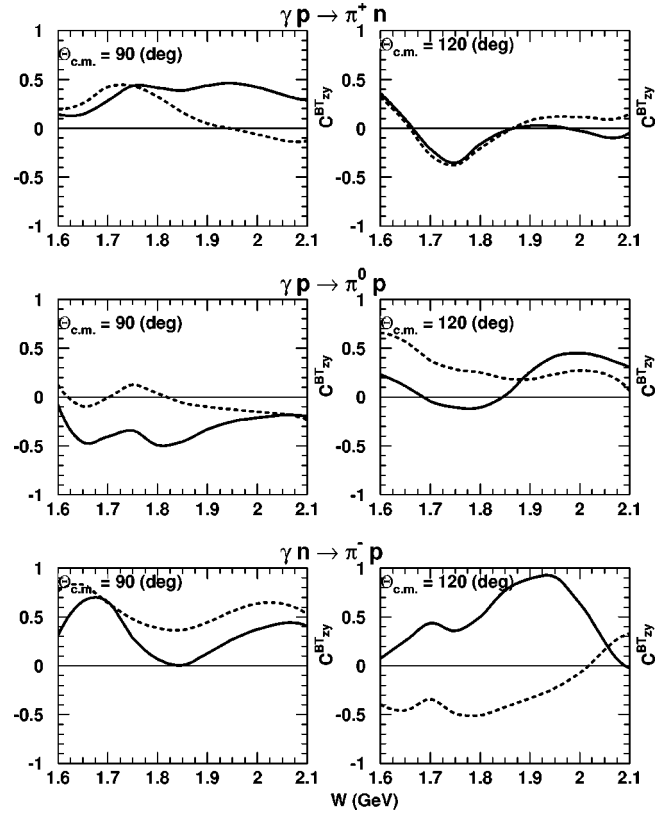
We now turn to reporting our investigations of the polarization observables. Before discussing the double polarization observables, we show in Fig. 2 some typical results from our calculations of single polarization observables. As expected, the effects due to nucleon resonances are much more visible here. Hopefully, these predictions can be tested in the near future when data from ongoing experiments becomes available.

To be more specific in our investigation of the double polarization observables, we focus on the most plausible experiments on beam-target and beam-recoil polarizations defined below:

$$C_{zy}^{BT} = \frac{\sigma^{(r,y;U,U)} - \sigma^{(r,-y;U,U)}}{\sigma^{(r,y;U,U)} + \sigma^{(r,-y;U,U)}}, \quad (10)$$

$$C_{zy}^{BR} = \frac{\sigma^{(r,U;y,U)} - \sigma^{(r,U;-y,U)}}{\sigma^{(r,U;y,U)} + \sigma^{(r,U;-y,U)}}, \quad (11)$$

where $\sigma^{(B,T;R,M)}$ is the cross section $d\sigma/d\Omega$ and the superscripts $(B,T;R,M)$ denote the polarizations of the beam, target and recoil, meson, respectively. r corresponds to a circularly polarized photon beam with helicity $+1$, $\pm y$ represents the direction of the nucleon polarization, and U represents the unpolarized particle. The coordinate system is chosen
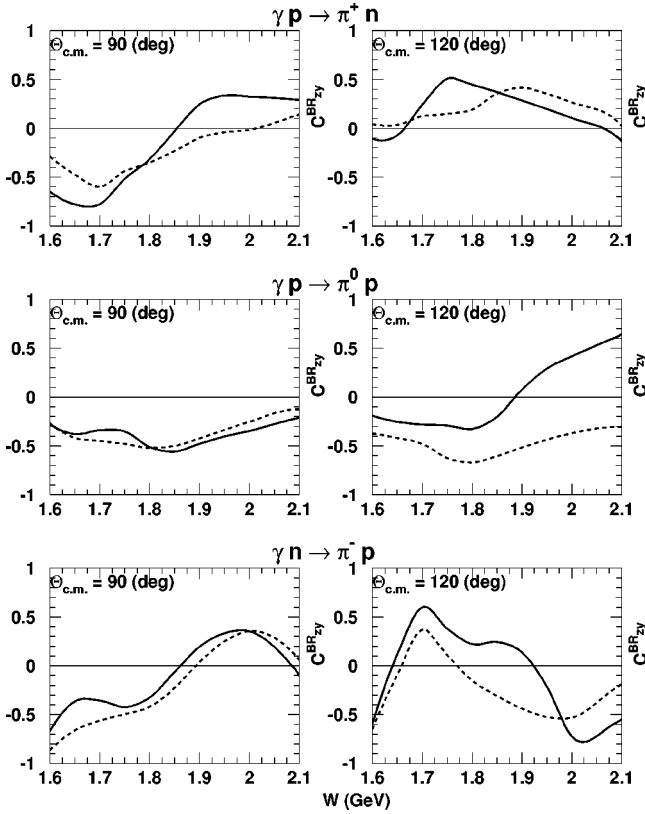
FIG. 4. Same as Fig. 3 except for the beam-recoil polarization C_{zy}^{BR}.

FIG. 5. The beam-recoil polarization C_{zy}^{BR} with photon helicity $= +1$ at c.m. angle 120°. The solid curves are from the SAID amplitude. The dashed curves are from the background amplitude + four-star resonances. The dot-dashed curves are from the background amplitude + four-star resonances + $N_{3/2}^-(1960)$.

such that the incoming photon is in the z direction and x-z plane is the reaction plane. Thus the y direction is perpendicular to the reaction plane.

We have performed extensive calculations of the two double polarization observables C_{zy}^{BT} and C_{zy}^{BR} in the energy region 1.6 GeV$<W<$2.1 GeV. As expected, the resonance effects are much more pronounced than what can be observed in Fig. 1 for the unpolarized cross section, and Fig. 2 for the single polarization observables. This is illustrated in Fig. 3 for the beam-target polarization and Fig. 4 for the beam-recoil polarization for two typical angles at 90° and 120°.

Our next task is to explore the favorable kinematic regions where only one or just a limited number of nucleon resonances among the 56 considered resonance states will be dominant. We have found that at angles close to 120° the resonance effects on the beam-recoil polarization [Eq. (11)] are mainly due to the four-star resonances $N_{9/2}^+(2345)$ of Table I and $N_{7/2}^-(2090)$ and $N_{9/2}^-(2215)$ of Table II, and the two-star resonance $N_{3/2}^-(1960)$ of Table II. Furthermore, the $N_{3/2}^-(1960)$ state has the largest effect among about 50 two-star and missing resonances in this higher-energy region. This is shown in Fig. 5. We see that by adding only the two-star $N_{3/2}^-(1960)$ to the calculation including only background and three four-star resonances, the predicted beam-recoil polarizations are shifted from the dashed curves to the
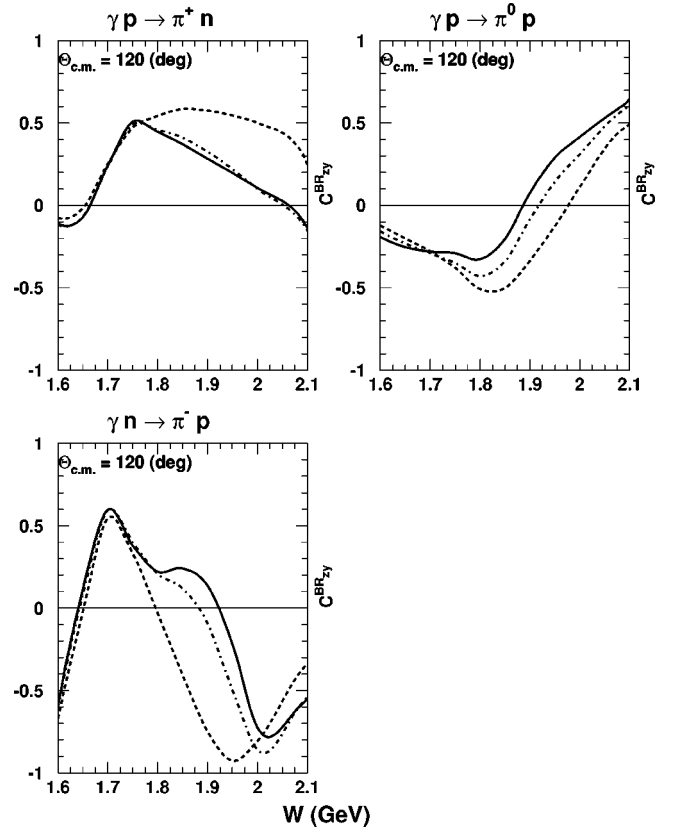
dot-dashed curves which are close to the results from full calculations including all resonances listed in Tables I–IV. The investigation of the two-star $N_{3/2}^-(1960)$ is clearly most favorable in the $\gamma p \to \pi^+ n$ channel.

Our results suggest that data on the double polarization observables of pion photoproduction in the region $1.6 \leq W \leq 2.1$ GeV could be very useful in investigating nucleon resonances. The experiments on these observables would be complementary to other similarly motivated ongoing experiments on vector meson photoproduction and kaon photoproduction. Moreover, these double polarization observables should be accessible at facilities such as Jefferson Lab and Spring-8. To end, we would like to mention that some experimental data on double polarization observables have recently become available in the $\gamma p \to \pi^0 p$ channel for $W > 1.6$ GeV [14], but there are no data on the other two charged channels.

[1] R. Koniuk and N. Isgur, Phys. Rev. D **21**, 1868 (1980).

[2] Q. Zhao, Z. Li, and C. Bennhold, Phys. Lett. B **436**, 42 (1998); Phys. Rev. C **58**, 2393 (1998).

[3] Q. Zhao, J.-P. Didelez, M. Guidal, and B. Saghai, Nucl. Phys. **A660**, 323 (1999).

[4] Yongseok Oh, A. I. Titov, and T.-S. H. Lee, Phys. Rev. C **63**, 025201 (2001).

[5] D. Sober, JLab Propoal No. 91-015 (unpublished); W. Briscoe *et al.*, JLab Proposal No. 94-103 (unpublished).

[6] T. Sato and T.-S. H. Lee, Phys. Rev. C **54**, 2660 (1996).

[7] S. Capstick, Phys. Rev. D **46**, 2864 (1992).

[8] S. Capstick and W. Roberts, Phys. Rev. D **49**, 4570 (1994).

[9] R. A. Arndt, I. I. Strakovsky, and R. L. Workman (unpub-lished). We use the Summer 2001 (SM01) solution from the SAID program available at http://gwdac.phys.gwu.edu

[10] Z. Li, Ph.D. thesis, Virginia Polytechnic Institute and State University, 1992.

[11] T. Yoshimoto, T. Sato, M. Arima, and T.-S. H. Lee, Phys. Rev. C **61**, 065203 (2000).

[12] Particle Data Group, C. Caso *et al.*, Eur. Phys. J. C **3**, 1 (1998).

[13] S. Capstick (private communication).

[14] R. Gilman and R. J. Holt, JLab Proposal No. E89-019; R. Gilman, R. J. Holt, and K. Wijesooriya (private communication).

[15] HEPDATA Reaction Database available at http://durpdg.dur.ac.uk/HEPDATA/REAC